

Electronic Supplementary Information

Sensitive CVG-AFS / ICP-MS label-free nucleic acids and proteins assays based on selective cation exchange reaction and simple filtration separation

Piaopiao Chen,^a Ke Huang,^b Rui Dai,^b Erica Sawyer,^a Ke Sun,^a Binwu Ying,^a Xiawei Wei^a
and Jia Geng^{*a}

^a Department of Laboratory Medicine, State Key Laboratory of Biotherapy and Cancer
Center, West China Hospital, Sichuan University and Collaborative Innovation Center for
Biotherapy, Chengdu, Sichuan, 610041, China

^b College of Chemistry and Material Science, Sichuan Normal University, Chengdu,
Sichuan, 610068, China

*Corresponding author. E-mail: geng.jia@scu.edu.cn

Table S1 Operational parameters of atomic fluorescence spectrometer (AFS)

Parameters	Value
Sampling time (s)	8
PMT high voltage (V)	-250
Carrier gas flow rate (mL/min)	400
Shielded gas flow rate (mL/min)	800
Observation height (mm)	8
Reading time (s)	7
Delayed time (s)	2
Cd hollow cathode lamp current (mA)	60
Pump rotation (r/min)	100

Table S2 Operational parameters of ICP-MS

Parameters	Value
Radiofrequency power	1550 W
Coolant argon gas flow rate	1 mL/min
Carrier (nebulizer) gas flow rate	15 mL/min
Auxiliary argon gas flow rate	1 mL/min
Scanning mode	Peak area
Dwelling time	40 s
Isotope monitored	Cd ¹¹¹

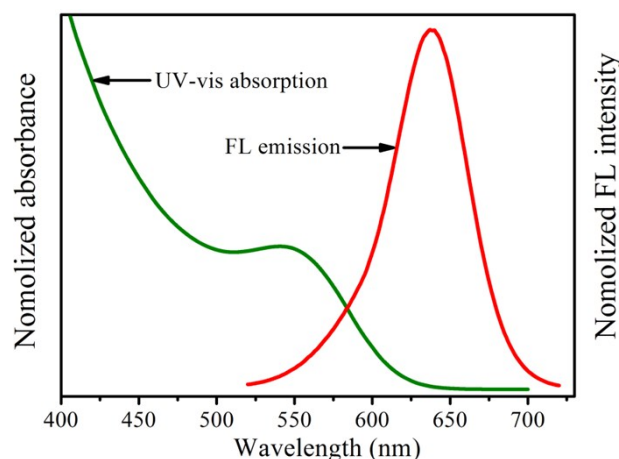


Fig. S1 The spectra of the UV-vis absorption (green curve) and the fluorescence emission (FL, red curve) of the CdTe QDs.

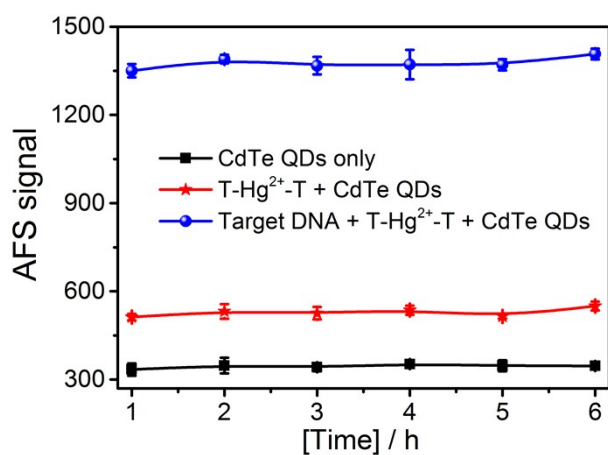


Fig. S2 The stability testing experiment.

Optimization of selective cation exchange reaction conditions

The appropriate selective cation exchange reaction time between Hg²⁺/ T-Hg²⁺-T with CdTe QDs was investigated. The AFS signal increased rapidly with increasing incubation time from 0 to 75 min and then leveled off after 75 min (as shown in Fig. S3A). Consequently, an incubating time of 75 min was adopted for the cation exchange reaction.

The amount of CdTe QDs is an important parameter for this work. It was found

that the AFS signal difference (Hg^{2+} + CdTe QDs and CdTe QDs) decreased significantly with increasing the dilution rate of CdTe QDs from 15 to 30 (as shown in Fig. S3B). Therefore, 15 times diluted CdTe QDs was ultimately selected for subsequent experiments.

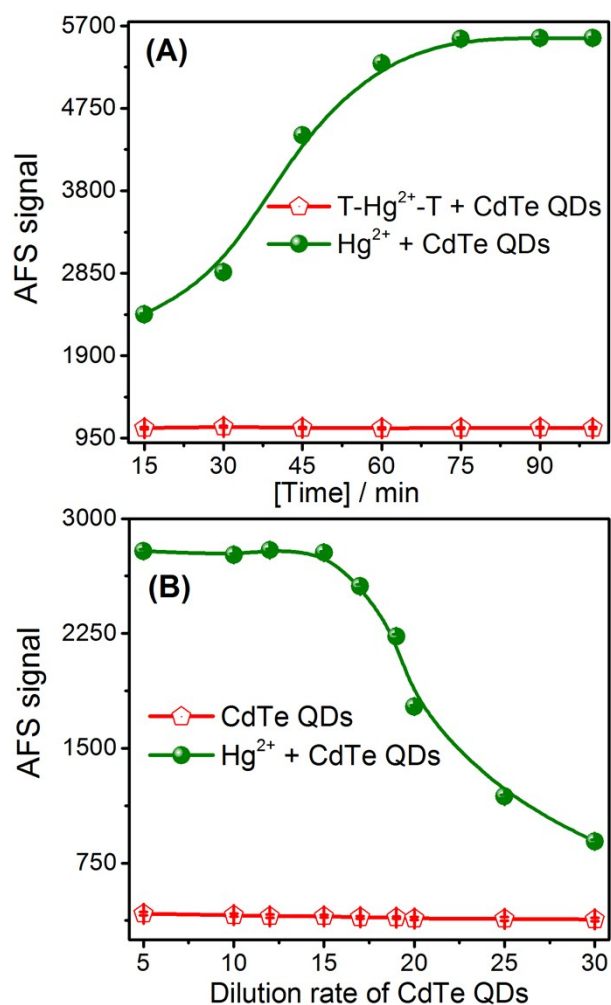


Fig. S3 Optimization of the selective cation exchange reaction conditions: (A) the reaction time between CdTe QDs and Hg^{2+} . (B) The amount of CdTe QDs. Error bars were estimated from three replicate measurements.

Formation T-Hg²⁺-T conditions for target DNA detection

The different molar ratios of P1-DNA to Hg^{2+} were investigated (Fig. S4A). The optimal molar ratio of P1-DNA to Hg^{2+} is 1:6 in this method. These experimental

results well agree with the previous report. Based on these results, concentrations of 40 nM of P1-DNA and 0.24 μM of Hg^{2+} were selected for further studies.

Besides, incubation time is important for the formation of T- Hg^{2+} -T hairpin structure. As shown in Fig. S4B, the reaction between P1-DNA and Hg^{2+} could reach the equilibrium within 60 min. Hence, the incubation time of 1 h was selected for further experiments.

It is known that Mg^{2+} can not only accelerate the combined rate between T-rich DNA and Hg^{2+} to form the T- Hg^{2+} -T hairpin structure, but also stabilize the DNA structure due to neutralized negatively charged phosphate group. As shown in Fig. S4C, the optimal concentration of Mg^{2+} is 12 mM in this target DNA detection method.

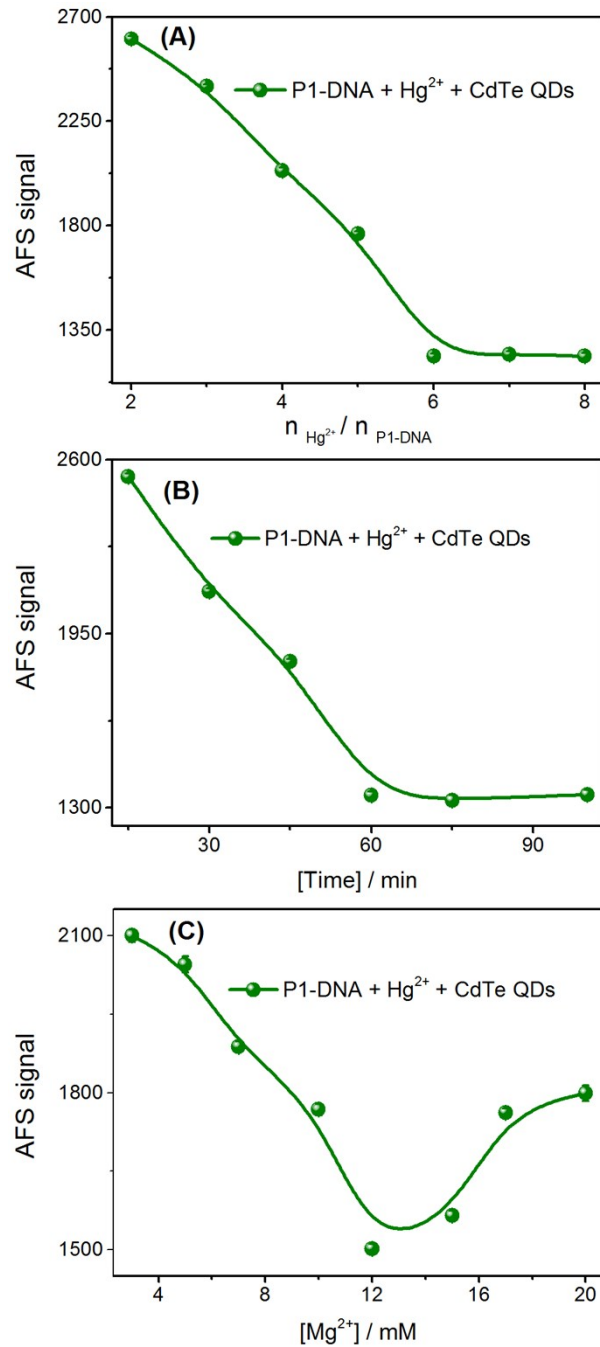


Fig. S4 The parameters that influence the formation of the T-Hg²⁺-T hairpin structure for DNA detection. (A) Concentration ratio of Hg²⁺ and probe 1 DNA. (B) Incubation time between probe 1 DNA and Hg²⁺. (C) The concentration of Mg²⁺ in the PBS buffer. Error bars were estimated from three replicate measurements.

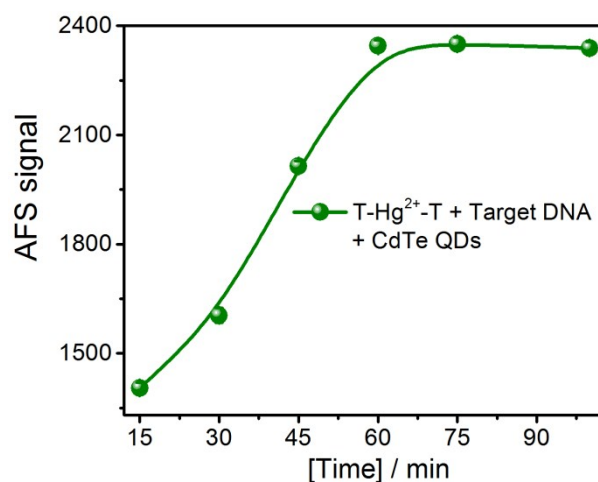


Fig. S5 The reaction time of the hybridization between the T-Hg²⁺-T and the target DNA. AFS signal of the solution containing 10 nM T-Hg²⁺-T and 10 nM target DNA. Error bars were estimated from three replicate measurements.

The competition reaction time between T-Hg²⁺-T and target DNA

We also studied the appropriate competition reaction time for the competition reaction between the target DNA with the P1-Hg²⁺ complex. The AFS signals increased rapidly with increasing incubation time from 0 to 2 h and then leveled off after 1 h (as shown in Fig. S5). Consequently, an incubating time of 1 h was adopted for the competition reaction.

Table S3 Comparison of different strategies for the detection of DNA

Method	System	LOD	Reference
Fluorescence	Aggregation-induced emission (AIE)	0.17 nM	1
Colorimetric	Au NPs- hemin/G-quadruplex	4.5 nM	2
Electrochemical	Hexavalent Chromium	1 nM	3
Quartz crystal microbalance (QCM)	DNA-streptavidin nanostructure	23 pM	4
Fluorescence anisotropy	Graphene oxide (GO)	4.6 nM	5
ICP-MS ^a	Double-strand DNA templated Cu NPs	4 pM	6
CE-ICP-MS ^b	T-Hg ²⁺ -T	8 nM	7
CVG-AFS ^c	T-Hg ²⁺ -T	0.2 nM	8
AAS ^d	Au NPs	0.23 nM	9
CVG-AFS / ICP-MS	T-Hg ²⁺ -T / CdTe QDs	0.2 nM	This work

^a Inductively coupled plasma mass spectrometry, ^b capillary electrophoresis-inductively coupled plasma mass spectrometry, ^c cold vapor generation-atomic fluorescence spectrometry, ^d atomic absorption spectrometry.

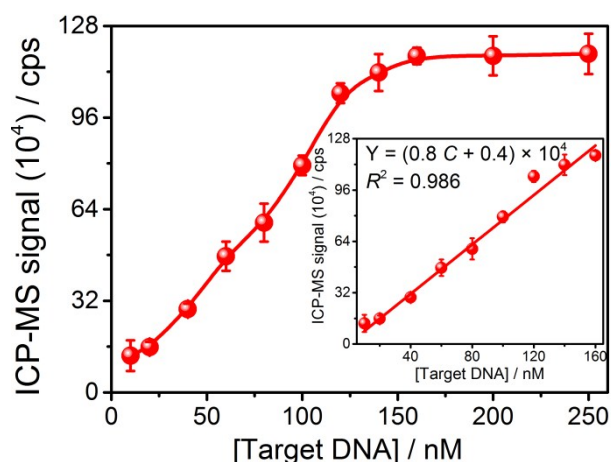


Fig. S6 Analytical performance of the proposed method based on the selective cation exchange reaction and simple filtration separation for DNA detection with ICP-MS used as the detector. Error bars were estimated from three replicate measurements.

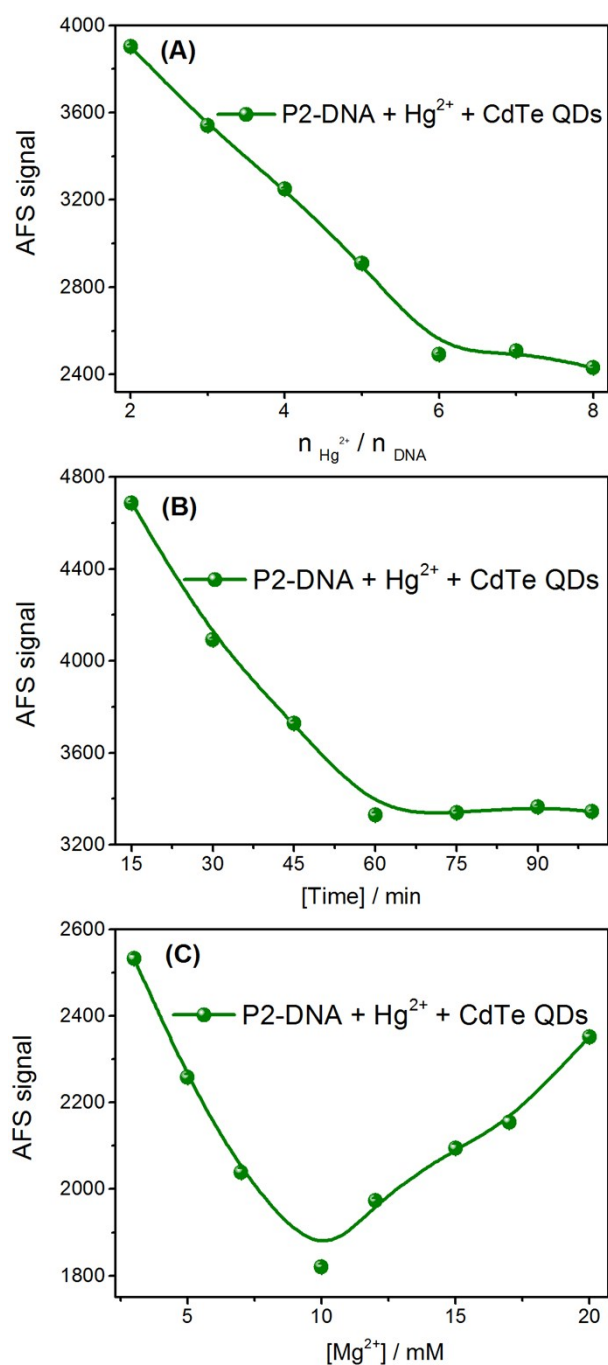


Fig. S7 The parameters that influence the formation of the T-Hg²⁺-T hairpin structure for CEA detection. (A) Concentration ratio of Hg²⁺ and probe 2 DNA. (B) Incubation time between probe 2 DNA and Hg²⁺. (C) The concentration of Mg²⁺ in the PBS buffer. Error bars were estimated from three replicate measurements.

The formation of T-Hg²⁺-T hairpin structure for CEA detection

The different molar ratio between P2-DNA and Hg²⁺ were investigated (Fig. S7A).

The optimal molar ratio of P2-DNA and Hg^{2+} is 1:6 in this method. Based on the results, 40 nM of aptamer and 240 nM of Hg^{2+} concentration were selected for the further studies.

Incubation time is important for the formation of T- Hg^{2+} -T hairpin structure, and its effect was investigated from 15 min to 100 min. As shown in Fig. S7B, the reaction between the P2-DNA and Hg^{2+} can reach the equilibrium within 1 h. Hence, the incubation time of 1 h was selected for further experiments.

The effect of Mg^{2+} concentration on the formation of T- Hg^{2+} -T structure was also investigated. As shown in Fig. S7C, when the concentration of Mg^{2+} was 10 mM, the AFS signal was the lowest.

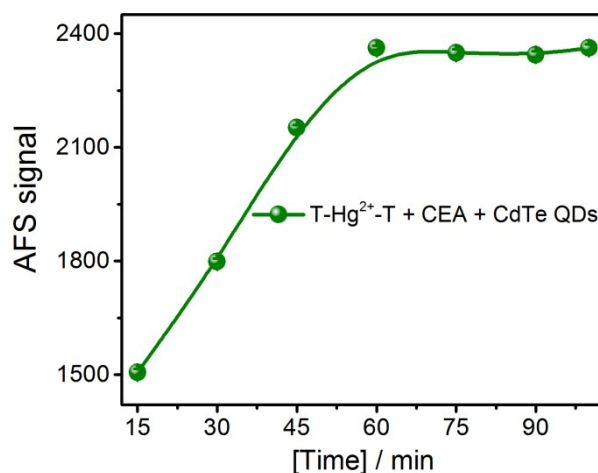


Fig. S8 The competitive reaction time between the T- Hg^{2+} -T hairpin structure (P2-DNA + Hg^{2+}) and CEA. AFS signal of the solution containing 10 nM T- Hg^{2+} -T and 10 ng/mL target CEA. Error bars were estimated from three replicate measurements.

Competition reaction time between P2-DNA and CEA

We also studied the appropriate time for the competition reaction between the target CEA with the T- Hg^{2+} -T complex. The AFS signal increased rapidly with

incubation time from 0 to 100 min and then leveled off after 60 min (as shown in Fig. S8). Consequently, an incubating time of 1 h was adopted for the competition reaction.

Table S4 Comparison of different strategies for the detection of CEA

Method	System	LOD	Reference
Fluorescence	QDs-tagged photonic crystal beads	0.89 ng/mL	10
Chemiluminescence	Dual-functional cupric oxide nanorods	0.05 ng/mL	11
Colorimetric	Iron oxide magnetic nanoparticle	3.6 pg/mL	12
Electrochemical	Mg ²⁺ -dependent MNAzyme	1.5 pg/mL	13
Photoelectrochemical	NaYF ₄ :Yb,Tm@TiO ₂ upconversion microrods with rolling circle amplification (RCA)	3.6 pg/mL	14
SPR ^a	AgNCs@Apt@UiO-66	0.3 ng/mL	15
SERS ^b	NiFe@Au	0.1 pM	16
SELDI-TOF MS ^c	Antibody-modified phospholipid bilayer coated gold nanoparticles	0.2 ng/mL	17
CVG-AFS / ICP-MS	T-Hg ²⁺ -T / CdTe QDs	0.2 ng/mL	This work

^a Surface plasmon resonance, ^b surface enhanced Raman scattering, ^c surface enhanced laser desorption ionization-time of flight mass spectrometry.

References

- 1 H. Wang, K. Ma, B. Xu and W. J. Tian, *Small*, 2016, **12**, 6613-6622.
- 2 A. Niazov-Elkan, E. Golub, E. Sharon, D. Balogh and I. Willner, *Small*, 2014, **10**, 2883-2891.
- 3 H. R. Lotfi Zadeh Zhad and R. Y. Lai, *Anal. Chem.*, 2017, **89**, 13342-13348.
- 4 Y. Zhao, H. M. Wang, W. Tang, S. C. Hu, N. Li and F. Liu, *Chem. Commun.*, 2015, **51**, 10660-10663.
- 5 X. Xiao, Y. F. Li, C. Z. Huang and S. J. Zhen, *Chem. Commun.*, 2015, **51**, 16080-16083.
- 6 R. Liu, C. Q. Wang, Y. M. Xu, J. Y. Hu, D. Y. Deng and Y. Lv, *Anal. Chem.*, 2017, **89**, 13269-13274.
- 7 Y. Li, S. K. Sun, J. L. Yang and Y. Jiang, *Analyst*, 2011, **136**, 5038-5045.

- 8 P. P. Chen, P. Wu, J. B. Chen, P. Yang, X. F. Zhang, C. B. Zheng and X. D. Hou, *Anal. Chem.*, 2016, **88**, 2065-2971.
- 9 H. Zhang, Z. F. Zhu, Z. X. Zeng and L. S. Ling, *J. Anal. At. Spectrom.*, 2014, **29**, 1591-1597.
- 10 J. Li, H. Wang, S. J. Dong, P. Z. Zhu, G. W. Diao and Z. J. Yang, *Chem. Commun.*, 2014, **50**, 14589-14592.
- 11 J. Li, Y. Cao, S. S. Hinman, K. S. McKeating, Y. W. Guan, X. Y. Hu, Q. Cheng and Z. J. Yang, *Biosens. Bioelectron.*, 2018, **100**, 304-311.
- 12 Z. Y. Zhang, J. Xie, J. Yu, Z. S. Lu and Y. S. Liu, *J. Mater. Chem. B.*, 2017, **5**, 14541460.
- 13 K. W. Ren, J. Wu, H. X. Ju and F. Yan, *Anal. Chem.*, 2015, **87**, 16941700.
- 14 Z. L. Qiu, J. Shu and D. P. Tang, *Anal. Chem.*, 2017, **90**, 1021-1028.
- 15 C. P. Guo, F. F. Su, Y. P. Song, B. Hu, M. H. Wang, L. H. He, D. L. Peng and Z. H. Zhang, *ACS Appl. Mater. Interfaces*, 2017, **9**, 41188-41199.
- 16 J. Li, Z. Skeete, S. Y. Shan, S. Yan, K. Kurzatkowska, W. Zhao, Q. M. Ngo, P. Holubovska, J. Luo and M. Hepel, *Anal. Chem.*, 2015, **87**, 10698-10702.
- 17 X. C. Lin, X. N. Wang, L. Liu, Q. Wen, R. Q. Yu and J. H. Jiang, *Anal. Chem.*, 2016, **88**, 9881-9884.